

Spin-dependent quantum transport in periodic magnetic modulations: Aharonov-Bohm ring structure as a spin filter

M. W. Wu,^{1,2,*} J. Zhou,² and Q. W. Shi¹

¹Hefei National Laboratory for Physical Sciences at Microscale,
University of Science and Technology of China, Hefei, Anhui, 230026, China

²Department of Physics, University of Science and Technology of China, Hefei, Anhui, 230026, China[†]
(Dated: October 30, 2018)

Quantum interference in Aharonov-Bohm (AB) ring structure provides additional control of spin at mesoscopic scale. We propose a scheme for spin filter by studying the coherent transport through the AB structure with lateral magnetic modulation on both arms of the ring structure. Large spin polarized current can be obtained with many energy channels.

PACS numbers: 85.75.-d, 73.23.Ad, 72.25.-b

Spin-based devices hold promises for future applications in conventional as well as in quantum computer hardware.^{1,2,3} Spin injection across interfaces is one of the crucial ingredients for such applications. However, an efficiency of spin injection through ideal ferromagnet/non-magnetic semiconductor interfaces is disappointingly small due to the large conductivity mismatch⁴ between the magnetic ferromagnet and the semiconductor. The use of spin filters⁵ is therefore an alternative approach which can significantly enhance spin injection efficiencies. In most of these works, spin-selective barriers or stubs⁶ are essential to realize the spin polarization (SP). Recently we propose a scheme for spin filters that the SP is generated during the transport through quantum wires with periodic lateral magnetic modulation which is much *weaker* than the Fermi energy E_f of the leads (Electrons therefore transport without tunneling through any barrier or being mode-selected by any stub). 100 % SP through the filter is predicted which originates from the mismatch of the effective spin-band-gaps induced by the Bragg-diffraction from the periodic modulation.⁷ The spin current density is up to 5.45 nA. However there is only one fixed energy interval for such SP.

In this letter we propose an improved design of the spin filter in the Aharonov-Bohm (AB) ring structure,⁸ an AB frame, coupled symmetrically to two leads to further increase the SP (by one order of magnitude) and the energy intervals (channels) for the SP by the additional degree of freedom, *ie.* the AB flux. A schematic of the spin filter is shown in Fig. 1. A periodic spin dependent modulation with Zeeman-like form $V_\sigma(x, y) = \sigma V_0 g(x, y)$ is applied symmetrically along both arms of the microstructure. Here $g(x, y) = 1$ if (x, y) locates at the gray areas (A layers), and 0 otherwise. σ is ± 1 for spin-up and -down electrons respectively. V_0 denotes a spin-independent parameter for the strength of the potential. This modulation can be realized by sticking magnetic strips on top of the sample or using magnetic semiconductor as the A layer. For $E_f \gg V_0$, spin-up and -down electrons experience different potentials: the spin-up electrons coherently transport under the modulation of the “transparent” barriers on the arms while the spin-down ones do under the

modulation of wells. The AB flux through the AB frame is introduced by a homogeneous magnetic field B . For the sake of simplicity for the experimental realization, we assume this magnetic field is applied not only inside the frame, but also on the arms.

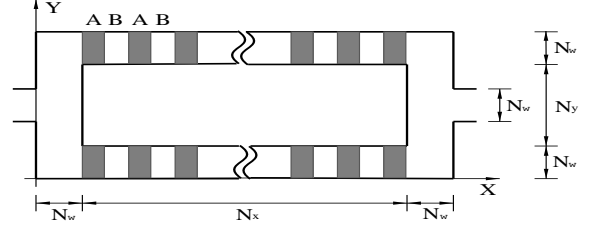


FIG. 1: Schematic of the spin filter in AB ring structure.

We describe the AB frame by a tight-binding Hamiltonian with the nearest-neighbour approximation:

$$H = \sum_{l,m,\sigma} \left(\frac{\epsilon_{l,m,\sigma}}{2} c_{l,m,\sigma}^\dagger c_{l,m,\sigma} + t_{l,m+1;l,m} c_{l,m+1,\sigma}^\dagger c_{l,m,\sigma} + t_{l+1,m;l,m} c_{l+1,m,\sigma}^\dagger c_{l,m,\sigma} + \text{H.C.} \right), \quad (1)$$

in which l and m denote the coordinates along the x - and y -axis respectively. $\epsilon_{l,m,\sigma} = \epsilon_0 + \sigma V_0$ ($= \epsilon_0$) when (l, m) locates at the gray (blank) areas of the frame, denotes the on-site energy with $\epsilon_0 = -4t_0$. $t_0 = -\hbar^2/(2m^*a^2)$ is the hopping energy with m^* and a standing for the effective mass and the “lattice” constant respectively. With the vector potential \mathbf{A} in the Landau gauge, *ie.*, $\mathbf{A} = (-\frac{1}{2}By, \frac{1}{2}Bx, 0)$, the hopping energy between $\mathbf{r}_i [= (l_i, m_i, 0)]$ and \mathbf{r}_j is given by $t_{\mathbf{r}_i, \mathbf{r}_j} = t_0 e^{[ie\mathbf{A} \cdot (\mathbf{r}_i - \mathbf{r}_j)/\hbar]}$.

The spin dependent conductance is calculated using the Landauer-Büttiker⁹ formula with the help of the Green function method.¹⁰ The two-terminal spin-resolved conductance is given by $G^{\sigma\sigma'} = (e^2/h) \text{Tr}[\Gamma_1^\sigma G_{1(2N_w+N_x)}^{\sigma\sigma'+} \Gamma_{2N_w+N_x}^{\sigma'} G_{(2N_w+N_x)1}^{\sigma'\sigma-}]$ with Γ_1 ($\Gamma_{2N_w+N_x}$) representing the self-energy function for the isolated ideal leads.¹⁰ We choose the perfect ideal ohmic contact between the leads and the semiconductor. $G_{1(2N_w+N_x)}^{\sigma\sigma'+}$ and $G_{(2N_w+N_x)1}^{\sigma'\sigma-}$ are the retarded and advanced Green functions for the conductor, but with the

effect of the leads included. The trace is performed over the spatial degrees of freedom along the y -axis. The spin dependent current within an energy window $[E, E + \Delta E]$ is given by $I_\sigma = \int_E^{E+\Delta E} G^{\sigma\sigma}(E)dE$.

We perform a numerical calculation for an AB frame with fixed arm width $N_w a = 20a$. A hard wall potential is applied in this transverse direction which makes the lowest energy of the n th subband (mode) be $\epsilon_n = 2|t_0|\{1 - \cos[n\pi/(N_w + 1)]\}$. The total length and width of frame are $500a$ and $90a$ respectively with $a = 9.53 \text{ \AA}$ throughout the computation. The length of A layer L_A is taken to be the same as that of B layer with $L_A = L_B = 8a$. We take the Zeeman splitting energy $V_0 = 0.001|t_0|$. Unless otherwise specified, $B = 0.45\phi_0/S$ with $S = (2N_w + N_x)(2N_w + N_y)a^2$ denoting the area of the AB frame and $\phi_0 = h/e$ standing for the quantum unit of flux. It is noted that $g\mu_B B \ll V_0$.

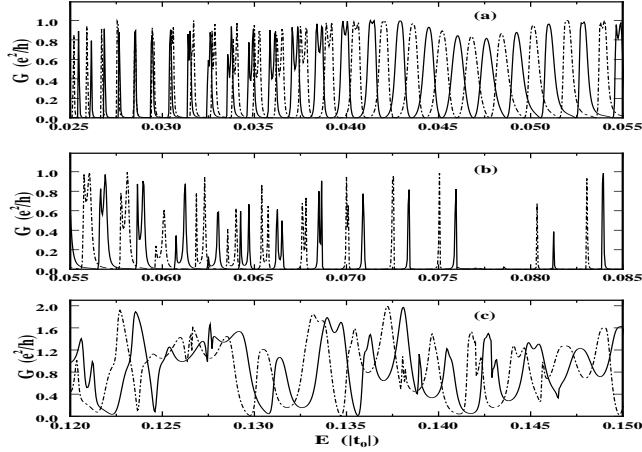


FIG. 2: Conductance versus the energy of the electron with (a) and (b) compose the first subband and (c) gives part of the second subband. Solid curve: $G^{\uparrow\uparrow}$; Chain curve: $G^{\downarrow\downarrow}$.

In Fig. 2 (a) and (b), the conductance is plotted as a function of the Fermi energy E of the leads, with E limited to the first subband. It is seen from the figure that for the AB ring structure with periodic magnetic modulations, due to the interference many energy windows are opened which give large SP, in contrast to the quantum wire where only *one* energy window is opened for large SP.⁷ The largest spin current density can be obtained from the energy window $[0.0566|t_0|, 0.0576|t_0|]$ with $I_\uparrow^{SP} = I_\uparrow - I_\downarrow \approx 16.8 \text{ nA}$ for spin-up current and from the window $[0.0556|t_0|, 0.0565|t_0|]$ with $I_\downarrow^{SP} = I_\downarrow - I_\uparrow \approx 13.4 \text{ nA}$ for spin-down current. A zero conductance of spin-up electron near $E = 0.06|t_0|$ corresponds to the energy gap due to the modulations predicted in 1D case, with the wave length of $\lambda \sim 2(L_A + L_B)$.⁷ A spin-independent gap between $0.075|t_0|$ to $0.08|t_0|$ origins from the interference effect of the four rectangular bends of the AB frame. By reshaping these four bends, we obtain the shift of this gap. Larger spin-current density can be obtained with multi-mode transport. In Fig. 2(c) we

plot the conductance versus the energy in the regime of the second subband and therefore two modes participate the carrier transport. By choosing the energy window $[0.1217|t_0|, 0.1234|t_0|]$, one gets the spin current density $I_\downarrow^{SP} = 43.6 \text{ nA}$.

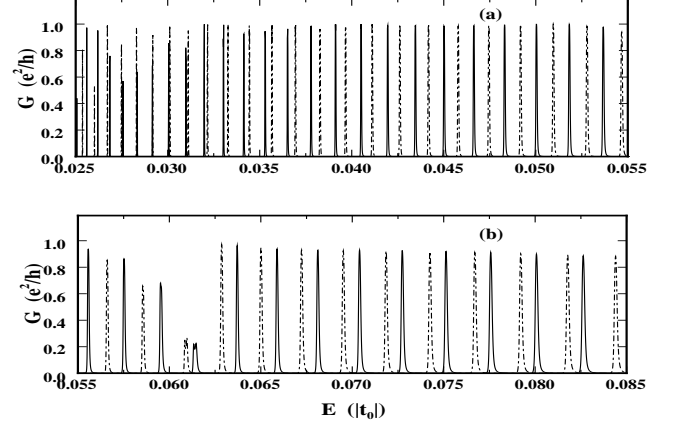


FIG. 3: Conductance versus the energy of the electron from the 1D model. Solid curve: $G^{\uparrow\uparrow}$; Chain curve: $G^{\downarrow\downarrow}$.

In order to further elucidate above features of the conductance, we simplify the AB frame by taking $N_w = 1$. Therefore one can solve the problem analytically with the approach developed by Xiong.¹¹ The Hamiltonian, including the leads can now be simplified as

$$\begin{aligned}
 H = & \sum_{N \geq i \geq 1\sigma} \epsilon_{\mu,i,\sigma} / 2 c_{\mu,i,\sigma}^\dagger c_{\mu,i,\sigma} + \sum_{\mu\sigma} \left[t_0 (c_{\mu,1,\sigma}^\dagger c_{L_0,\sigma} \right. \\
 & \left. + c_{R_0,\sigma}^\dagger c_{\mu,N,\sigma}) + \sum_{N > i \geq 1\sigma} t_{\mu,i+1;\mu,i} c_{\mu,i+1,\sigma}^\dagger c_{\mu,i,\sigma} \right] \\
 & + t_0 \sum_{j > 0\sigma} (c_{L_{-j+1,\sigma}}^\dagger c_{L_{-j,\sigma}} + c_{R_{j,\sigma}}^\dagger c_{R_{j-1,\sigma}}) + \text{H.C.} \quad (2)
 \end{aligned}$$

where $\mu = 1, 2$ denotes two arms and $i = 1 \dots N$ stands for the index of sites on each arm. L_j (R_j) labels the site of left (right) lead. Site index increases from the left to the right and two junctions between the leads and the arms are defined as the end of the leads denoted by L_0 and R_0 . We take the one-dimensional (1D) AB frame as the outer edge of the 2D structure in Fig. 1. Similar to the 2D problem, $\epsilon_{\mu,i,\sigma} = \epsilon'_0 + \sigma V_0$ (ϵ'_0) when i locates at A layer (otherwise). We take $\epsilon'_0 = \epsilon_1 + 2|t_0|$ where ϵ_1 is the lowest energy of the first subband and denote $E_{\mu,i,\sigma} = E - \epsilon_{\mu,i,\sigma}$ with E being the energy of the incident electron. The wave-function can be expressed as¹¹ $|\psi\rangle = [\sum_{j \geq 0,\sigma} (A_{L_{-j,\sigma}} c_{L_{-j,\sigma}}^\dagger + A_{R_{j,\sigma}} c_{R_{j,\sigma}}^\dagger) + \sum_{\mu,N \geq i \geq 1,\sigma} B_{\mu,i,\sigma} c_{\mu,i,\sigma}^\dagger] |0\rangle$, with the coefficients $A_{L_{j,\sigma}}$, $A_{R_{j,\sigma}}$ and $B_{\mu,i,\sigma}$ being determined from the Schrödinger equation $H|\psi\rangle = E|\psi\rangle$. By assuming a plane wave with unity amplitude and spin σ injected from the left lead, one has $A_{L_{j,\sigma}} = e^{ikj} + r_\sigma e^{-ikj}$ and $A_{R_{j,\sigma}} = t_\sigma e^{ikj}$ with r_σ and t_σ standing for the reflection and transmission amplitudes and k being the wave-vector satisfying

$2t_0 \cos k = E - \epsilon'_0$. The transmission coefficient $T_\sigma = |t_\sigma|^2$ is therefore given as

$$t_\sigma = \frac{-4i \sin k \cos(\frac{\phi}{2}) C_\sigma}{(2C_{N,\sigma} + e^{-ik})(2D_{N,\sigma} + e^{-ik}) - 4 \cos^2(\frac{\phi}{2}) C_\sigma D_\sigma}, \quad (3)$$

in which $C_{i,\sigma} = (E_{i,\sigma} - C_{i-1,\sigma})^{-1}$ with $C_{1,\sigma} = E_{1,\sigma}^{-1}$ and $D_{i,\sigma} = (E_{N-i+1,\sigma} - D_{i-1,\sigma})^{-1}$ with $D_{1,\sigma} = E_{N,\sigma}^{-1}$. $C_\sigma = \prod_{i=1}^N C_{i,\sigma}$ and $D_\sigma = \prod_{i=1}^N D_{i,\sigma}$.

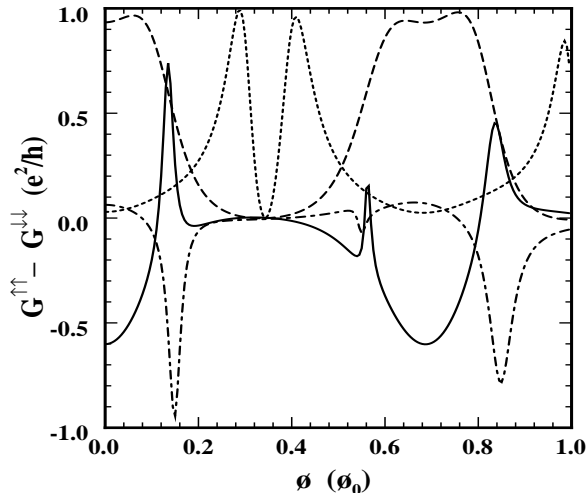


FIG. 4: $G^{\uparrow\uparrow} - G^{\downarrow\downarrow}$ versus the AB flux ϕ for different energies. Solid curve: $E = 0.0585|t_0|$; Dotted curve: $0.0589|t_0|$; Dashed curve: $0.0592|t_0|$; Chain curve: $E = 0.0595|t_0|$.

We apply the same magnetic field (and therefore the

AB flux) and use the same parameters as in the 2D case. The spin-dependent conductances $G^{\sigma\sigma} = (e^2/h)T_\sigma$ calculated from Eq. (3) are plotted in Fig. 3 and exhibit similar behavior as the 2D case in Fig. 2, including the band gap due to the magnetic modulation near $E = 0.06|t_0|$. However, the peaks of 1D structure is much narrower and the gap caused by the four rectangular bends in Fig. 2 disappears as the bends do not exist in the 1D problem.

Finally we consider the effect of AB flux. In Fig. 4, the difference of the conductances of spin-up and -down electrons of the 2D AB frame $G^{\uparrow\uparrow} - G^{\downarrow\downarrow}$ is plotted as a function of the flux ϕ for four typical energies: $E = 0.0585|t_0|$ (solid curve), $0.0589|t_0|$ (dotted curve), $0.0592|t_0|$ (dashed curve) and $0.0595|t_0|$ (chain curve). One finds efficient modulation due to the AB flux. Moreover, as the magnetic field is applied also on the arms of the AB frame, it is seen from the figure that the period is now roughly about $0.7\phi_0$, in contrast to ϕ_0 for the case when the flux is confined inside the frame.

In summary, we have proposed a scheme for spin filter by studying the coherent transport through an AB-ring structure with lateral magnetic modulation. Large SP is predicted and is shown to be accessible with many energy intervals. The magnetic modulation can be realized by sticking the magnetic strips on top of the sample or using magnetic semiconductor as A layers.

One of the authors (MWW) was supported by the ‘‘100 Person Project’’ of Chinese Academy of Sciences and Natural Science Foundation of China under Grant Nos. 9030312 and 10247002. He would like to thank S. J. Xiong for valuable discussions.

* Author to whom correspondence should be addressed; Electronic address: mwwu@ustc.edu.cn

† Mailing Address.

¹ G.A. Prinz, Phys. Today **48**, 58 (1995); Science **282**, 1660 (1998).

² D. Loss and D. P. DiVincenzo, Phys. Rev. A **57**, 120 (1998).

³ *Semiconductor Spintronics and Quantum Computation*, eds. D. D. Awschalom, D. Loss, and N. Samarth, Springer, Berlin, 2002.

⁴ G. Schmidt, D. Ferrand, L. W. Molenkamp, D. Ferrand, and L. W. Molenkamp, Phys. Rev. B **62**, R4790 (2000).

⁵ M.J. Gilbert and J.P. Bird, Appl. Phys. Lett. **77**, 1050 (2000); G. Papp and F.M. Peeters, Appl. Phys. Lett. **78**, 2148 (2001); J.C. Egues, C. Gould, G. Richter, and L. W. Molenkamp, Phys. Rev. B **64**, 195319 (2001); Takaaki Koga, Junsaku Nitta, Supriyo Datta, and Hideaki Takayanagi, Phys. Rev. Lett. **88**, 126601 (2002); J. Frans-

son, E. Holmström, I. Sandalov, and O. Eriksson, Phys. Rev. B **67**, 205310 (2003); X.F. Wang and P. Vasilopoulos, Appl. Phys. Lett. **80**, 1400 (2002); **81**, 1636 (2002).

⁶ F. Sols, M. Macucci, U. Ravaioli, and Karl Hess, Appl. Phys. Lett. **54**, 350 (1989).

⁷ J. Zhou, Q. W. Shi, and M. W. Wu, Appl. Phys. Lett. **84**, 365 (2004).

⁸ Y. Aharonov and D. Bohm, Phys. Rev. **115**, 485 (1969); D. Frustaglia, M. Hentschel, and K. Richter, Phys. Rev. Lett. **87**, 256602 (2001); M. Popp, D. Frustaglia, and K. Richter, Nanotechnology **14**, 347 (2003).

⁹ M. Büttiker, Phys. Rev. Lett. **57**, 1761 (1986).

¹⁰ S. Datta, *Electronic Transport in Mesoscopic Systems* (Cambridge University Press, New York, 1995).

¹¹ Shi-Jie Xiong and Ye Xiong, Phys. Rev. Lett. **83**, 1407 (1999); Shi-Jie Xiong, Phys. Lett. A **319**, 198 (2003).